Multi-material bronze-steel plain bearings produced by laser-directed energy deposition

Matteo Perini
ProM Facility of Trentino Sviluppo S.p.a., Rovereto, Italy, and
Alessia Teresa Silvestri
Department of Chemical, Materials and Industrial Production Engineering, University of Naples Federico II, Naples, Italy

Abstract

Purpose – This study aims to manufacture bimetallic bearings by achieving a sound deposition of bronze. Indeed, systems with rotating components use parts that reduce friction by allowing them to rotate freely. This is typically achieved with either rolling bearings or plain bearings. The last ones are usually made of self-lubricating materials, which may not excel in mechanical properties. An interesting alternative lies in bimetallic brass bearings, like bronze-steel combinations. However, they are limited in terms of available shapes and sizes due to challenges associated with the conventional manufacturing process.

Design/methodology/approach – This study addresses the problems of mechanical weakness and production limitations of conventional brass bearings by introducing the use of Hybrid Manufacturing techniques: Laser Directed Energy Deposition technology in combination with five-axis milling. Specifically, Cu89Sn11 was deposited on a C45 substrate by varying the number of layers, and based on the results obtained, two kinds of bimetallic bearings were produced.

Findings – The results of the one, two and five-layers samples indicate a sound deposition of Cu89Sn11, without defects such as detachments, cracks or porosities. The microhardness profile shows a decreasing trend from the substrate to the deposition zones. Bending and adhesion tests confirmed the excellent material bonding. Five-layers of Bronze were deposited on a C45 substrate to fabricate hemispherical and flat-face bearings.

Originality/value – This study validates the feasibility of expanding the new class of 3D-printed high-performance materials, highlighting the advantages of additive manufacturing technologies, such as the design and material mixing freedom, by manufacturing two kinds of bimetallic bearings.

Keywords Hybrid manufacturing, Directed energy deposition, Bimetallic, Bronze, Steel, Plain bearing

Paper type Research paper

1. Introduction

A bearing serves as a crucial component between two moving surfaces, facilitating their relative motion while minimizing wear and reducing friction. Plain bearings, which are typically composed of or lined with material that achieve the above mentioned purpose for sliding contact, play a key role in supporting components such as shafts and other rotating elements (PRATT, 1973; Zeidan and Herbage, 1991). Therefore, to accomplish the goal for which they are designed (reduction of friction and wear) plain bearings must be manufactured of materials characterized by a low coefficient of friction, as well as the ability to withstand significant mechanical stresses, potentially corrosive environments and high temperatures. In addition, the material of the plain bearing must not cause wear of the element with which it comes into contact, and therefore usually has a lower hardness (Pratt, 2001). In most cases, plain bearings are lubricated with oil or grease to ensure proper operation. The choice of the appropriate bearing material depends on the type, quality and quantity of the lubricant used. For example, composite-based bearings have been developed for operation without the need for external lubrication. Among the commonly used materials, bronze stands out for its antifriction characteristics and good wear properties. Typically, it is as an alloy of copper, tin, zinc and lead. Other materials in use include tin-based alloys (babbitt), aluminum and copper-based alloys, cast iron in the case of a rotating shaft with very high hardness (the cast iron-steel combination has a low coefficient of friction), graphite or copper-graphite alloys, polymers or composites (Polytetrafluoroethylene, Poly-ether ether ketone, Ultra-high-molecular-weight polyethylene, Polylactic acid (PLA) and nylon especially) (Hanon *et al.*, 2020; Pratt, 2001; Summer *et al.*, 2019).

This kind of components are usually manufactured by means sintering or casting and machining (Junghans *et al.*, 1996). The former produces products that are often highly porous, which presents advantages and disadvantages. Porosity allows lubricating oil to penetrate the cavities in the bearing, ensuring operation even without external lubrication and allowing the oil

The current issue and full text archive of this journal is available on Emerald Insight at: **https://www.emerald.com/insight/1355-2546.htm**

Rapid Prototyping Journal
30/11 (2024) 325–335
Emerald Publishing Limited [ISSN 1355-2546]
[DOI 10.1108/RPJ-10-2023-0382]

The authors want to acknowledge Prof. A. Squillace and the LABCAMP[2] laboratory (CeSMA – University of Naples "Federico II") for hosting and supporting part of the experimental activities.

Received 31 October 2023
Revised 17 June 2024
Accepted 7 October 2024

to remain longer in the contact area. However, this porosity also compromises mechanical properties, especially under impact loads when the pores act as zones of stress concentration zones, and under cyclic loads where the imperfections and pores potentially promote cracks formation and propagation due to notch effect. All these problems can be caused by impacts, misalignment of bushing and shaft axes or assembly errors (Wilson and Shone, 1983).

To compensate for the poor mechanical properties of bushings made by sintering and the poor tribological properties of bushings made by casting, bimetallic plain bearings are often used. These bearings consist of a sheet, usually of low-carbon steel, onto which a sheet of bronze or other bearing alloy is either sintered or welded through brazing. This bimetallic sheet is then calendered to produce the finished bushing, with the steel layer on the outside. The result is bearings that are much more robust, tougher and tolerant of cyclic loads than cast or sintered bronze bearings, which are suitable for high loads at medium to high angular velocities. However, this type of element also has numerous disadvantages (Sudhakar, 2002; Tallafuss and Johnston, 2018). First and foremost, the diameter of the bearing must necessarily be limited to allow the sintered bronze to contact the shaft, because the brittleness of the bronze layer itself means that the bimetal cannot be bent with a radius of curvature that is too small without causing cracks. The wall thickness of the bushings is also limited with increasing thickness for the same reason and because of the increasing difficulty in bending. Consequently, these methods result in large, thin bearings, which in turn are inadequate under significant loads.

Moreover, the nature of this production method makes it impossible to obtain "integral" bimetallic bearings, i.e. without a seam line between the ends of the twisted foil (a point of possible failure and discontinuity of support on the rotating shaft), with special shapes, grooves, slots for positioning and clamping and shoulders, making this type of component difficult to use even under axial load.

Furthermore, the difference in the coefficients of thermal expansion between copper and steel alloys makes neither bimetallic nor conventional bushings suitable for use in wide temperature ranges, especially for large diameters. Under such conditions, more expensive rolling bearings, sometimes even with ceramic components, are required.

Another issue is the occurrence of galvanic corrosion phenomena when steel, mild or alloy, comes into contact with bronze in the presence of water or moisture. Steel and copper alloys are quite far apart in the galvanic series, this makes steel vulnerable to corrosion when exposed to bronze in the presence of external moisture or when water is present in the lubricant, acting as an electrolyte.

Less commonly used methods include sputtering and electrochemical deposition. However, in the first case, like other high-energy hot coating methods, the substrate is subjected to intense temperature and mechanical actions (Ovchinnikov *et al.*, 2000), greatly altering its structure and properties; in the second case, the process is complicated and long, involving also a phase of surface preparation before the actual process (Valeeva *et al.*, 2012).

In this context, this research study aims to address the aforementioned issue using innovative hybrid manufacturing: Laser-Directed Energy Deposition (L-DED) and five-axis milling. L-DED belongs to the family of additive manufacturing (AM) technologies and uses a focused laser beam to melt metal powders as they are being deposited on a substrate, and it is gaining great attention both from the industry and academia for its several advantages, such as waste reduction, possibility to print complex geometry, multi-material components and so on; moreover, L-DED is used also for repairing and coating applications (Gibson *et al.*, 2015; Izadi *et al.*, 2020).

Indeed, bimetallic structures have attracted significant interest in both academia and industry (Joshi and Badheka, 2019; Li *et al.*, 2014; Topolski *et al.*, 2016). However, DED-based AM machines are equipped with multiple feeders for different feedstock materials, making bimetallic structure fabrication easier and enabling *in situ* mixing to create a smooth transition between the two metallic materials, with respect to the other AM machines (Bandyopadhyay *et al.*, 2022; Kannan *et al.*, 2023; Silvestri *et al.*, 2021). For example, Chen *et al.* studied the deposition of 316L stainless steel and, then, CuSn10 Tin-Bronze using selective laser melting (SLM) (Chen *et al.*, 2019). However, although SLM offers high dimensional accuracy and low surface roughness, there are several constraints related to this technology, such as the dimensions of the building volume chamber and the use of a customized machine equipped with a special feeding system to produce bimetallic samples. Moreover, as introduced before, L-DED allows for the repair and refurbishment of bearings in case of future failures without the need to replace them, promoting a more sustainable manufacturing system.

This study demonstrates the potential of L-DED technology as a compelling alternative for producing sliding brushing, ensuring the proper adhesion between the two materials, without affecting the mechanical properties of the single material.

2. Materials and methods

The material used for the depositions is Cu89Sn11, produced by Goodfellow. The powder particles were in the range of size between 50 and 150 μm, and characterized by a flowability of 16 (sec/50g) in conformity to the ASTM B213-20 standard (ASTM International, 2014). The substrate was made of C45 steel, and they were sandblasted and degreased with acetone before the deposition process.

DMG MORI^{TM} LASERTEC 65 3D hybrid machine (LT 65 3D hybrid, DMG MORI AG, Pfronten, Germany) was used for printing the samples. This machine is equipped with a fiber laser of wavelength 1020 nm, spot diameter of 3000 μm and power up to 2500 W. The nozzle used for this study is named COAX14 and has a stand-off distance of 13 mm. This system was used for fabricating the samples and the bearings in a local inert argon atmosphere. The bronze was deposited adopting the following process parameters: a travel speed of 1000 mm/min, a powder feed rate of 12 g/min, an initial laser power of 2200 W. Specimens were produced in three different configurations adding 1, 2 and 5 layers of CuSn11 on the C45 substrate. Even if the first layer was printed using 2200 W, the laser power was decreased starting from the second layer with a reduction of 200 W, till reaching 1600 W in the fourth layer. The associated CAD/CAM software (Siemens NX) was used for the design, particular attention is paid to the choice of the scanning strategy (see Figure 1). The scanning strategy adopted for the 1-, 2- and 5-layer samples is bidirectional, also known as Zig-Zag, with a step-over of 1.4 mm [Figure 1(a)].

Rapid Prototyping Journal
Volume 30 · Number 11 · 2024 · 325–335

Figure 1 Some scanning strategies available in the Siemens NX software for the printing process

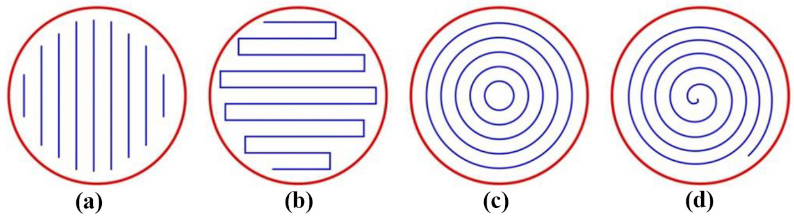

Notes: a) Zig; b) Meander; c) Concentric; d) Spiral
Source: Authors' own work

The starting point was rotated by 90 degrees between one layer and the next to avoid heat accumulation in the same region. The choice of zig-zag strategy is due to the square geometries of the samples. However, in the production of bearings, it is important to consider the geometries of the final item and the issue related to the material's thermal conductivity to be deposited, to avoid residual stresses and possible defects. To address this issue, some preliminary tests were carried out, and the spiral scanning strategy [Figure 1(d)] was found to be the most suitable deposition strategy for the final bushings designed, considering their circular shapes. The schematic of the adopted strategy is shown in Figure 2, where the red line represents the contour and consists of one single round of CuSn11 deposition, and the blue line represents the bulk strategy: the deposition head begins the spiral from the outside and then continues inward to the center. As in the previous cases, the step-over was set equal to 1.4 mm, and the starting point was rotated by 90 degrees layer by layer.

The deposited samples were cut and cross-sectioned via electrical discharge machining (EDM). Then, the specimens were hot-mounted in an acid-proof resin. The metallographic preparation has followed the metallographic procedure illustrated in Materials (2004).

Microhardness Vickers measurements have been conducted on the metallographic cross-sections with a load of 500 g and following the standard ASTM E92-82 [ASTM E92-82(2003), 2008].

In the one- and two- layers samples, due to the very small height of the cladding layer, it was possible to do the measurements with only one indentation along the vertical direction (i.e. building direction), and nine indentations in the horizontal one (i.e. deposition direction), with an inter-distance equal to 2 mm. Three indentations along the vertical direction and nine in the deposition direction were performed in the five-layers samples. Energy-dispersive X-ray spectroscopy (EDX) analyses were performed by means of an Electron Scanning Microscopy (SEM, Hitachi TM3000) equipped with an EDX probe.

Three-point bending and pull-off adhesion tests were performed to investigate the bonding strength between the materials. Three-point bending tests were carried out at room temperature using a universal testing machine (Galdabini QUASAR 50, Galdabini SPA, Italy) with a 50 kN load cell and 10 mm diameter support holders. The crosshead speed was set at 1 mm/min. The specimens had dimensions of 74 mm in length, 10 mm in width and 4 mm in thickness, consisting of 2 mm of C45 and 2 mm of CuSn11. The load was applied from the top. Tests were performed on two opposite positions of the sample, and three specimens were tested for each experimental condition: bronze at the top (indicated as "1B", "2B" and "3B" or as "B-samples"), and steel at the top (indicated as "1S", "2S" and "3S" or as "S-samples"). The support span was 64 mm, respecting the 16:1 span-to-thickness ratio (ASTM INTERNATIONAL, 2002), with an over-span of about 5 mm on each side.

The pull-off adhesive tests were performed following the ASTM D4541 standard using a PosiTest ATM (ASTM D454-22, 2022). An aluminum dolly with a 14 mm diameter was bonded to the top surface of the bronze deposits using cyanoacrylate glue (Figure 3). The coating consisted of five layers of bronze, which were machined after the deposition to

Figure 2 Schematic representation of the spiral scanning strategy used for the bearings manufacturing

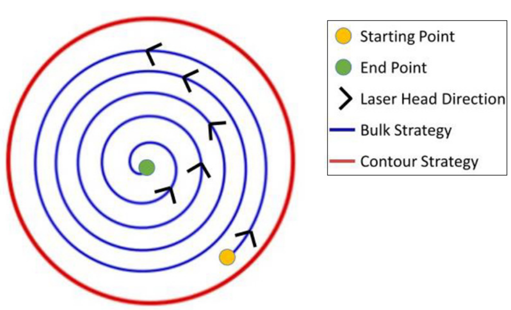

Source: Authors' own work

Figure 3 Schematic representation of the pull-off adhesive test

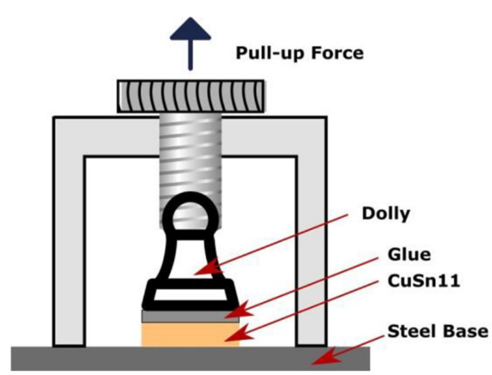

Source: Authors' own work

reach a planar surface, as recommended by the standard. The test was performed five times.

After the deposition and based on the analyses of the three abovementioned samples, two different models of brass bearings were manufactured through L-DED, using the same processing parameters introduced before.

The first model is a hemispherical bearing that needs to withstand very high loads, while the second one has a flat-face shape. In both models, some holes allow the lubricant to reach the contact surface, decreasing the friction force. The deposition of five layers of bronze for the bearings took around 20 min; then, after a few minutes of cooling down, by re-machining stock thickness (1 mm) we were able to obtain the final shape of the plain bearings. Other milling operations were performed to create features for the lubricant, such as the central hole in the hemispherical bearing. The components were then thoroughly cleaned in an ultrasonic bath.

It is important to highlight that the same machine used for the deposition was also used for the milling process to finish the components by machining without the need to change the computer numerical control (CNC) machine.

3. Results and discussions

The samples printed with one, two and five layers of CuSn11 are shown in Figure 4.

The first results of the microhardness analysis are presented in Figure 5. The one-layer cladding has a mean value of 176 HV, the two-layers sample shows a very close value, i.e. 177 HV and, finally, a slight reduction was detected in the five-layers sample, characterized by a microhardness of 158 HV.

The major size of the last sample allows a wider number of indentations on the cross-section, obtaining a more accurate microhardness profile (shown in Figure 6) from the substrate to the bronze deposition, through the interfacial region. In Figure 6, it is possible to note that the microhardness slightly decreases from the typical microhardness values of C45 in the steel region to the typical values of bronze in the CuSn11 region (Chen *et al.*, 2019), specifically from about 250 to 155 HV, going through 170–180 HV in the interfacial region. The intermediate values found in the interfacial region are strongly connected to the complex phenomena concerning the L-DED that led to a mixing of the substrate and deposited materials, mainly due to the Marangoni effect (Silvestri *et al.*, 2023; Thompson *et al.*, 2015). This mixing

Figure 4 CuSn11 Samples

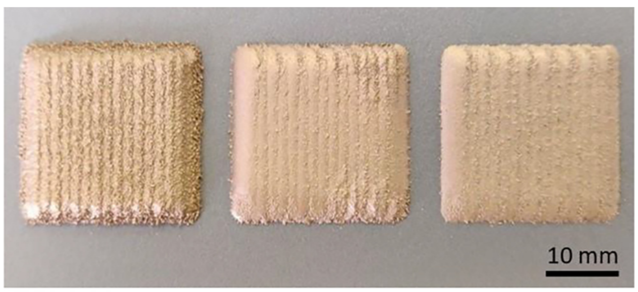

(a) (b) (c)

Notes: (a) Five-Layer; (b) Two-Layer; (c) One-Layer
Source: Authors' own work

Figure 5 Vickers microhardness measured along the cross-section of the samples: mean values and standard deviations

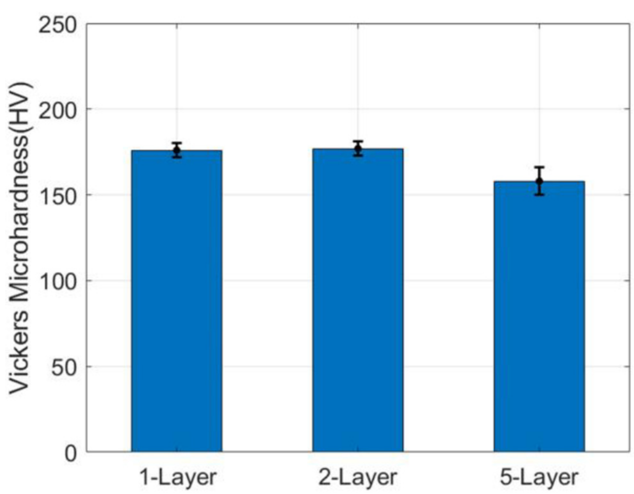

Source: Authors' own work

Figure 6 Vickers microhardness profile in the five-layer samples along the steel/bronze interface

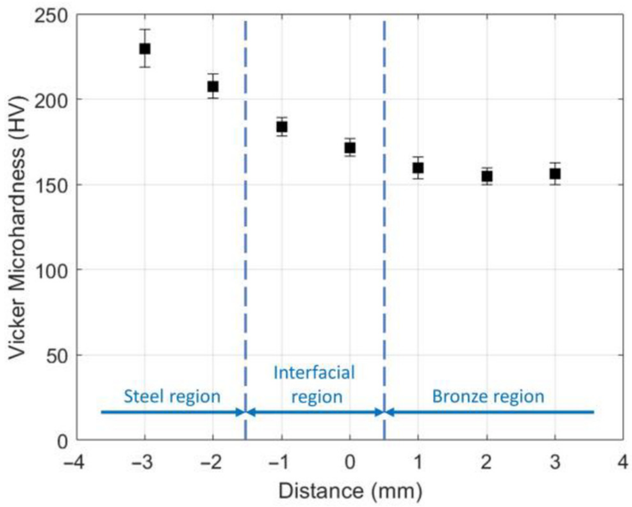

Source: Authors' own work

was confirmed by the EDX analysis, as explained below. Moreover, it is now possible to understand the reason why the mean values of Figure 5, discussed before, decrease from the one/two-layers samples (176–177 HV) to the five-layers samples (158 HV): it is possible to compare the zones analyzed in the first two cases to the "interfacial region" of the five-layers sample, characterized by the presence of the steel in the bronze layer and vice versa.

Indeed, in the one- and two- layers samples, due to the very small height of the cladding layer, measurements were possible with only one indentation along to the vertical direction (i.e. building direction), and nine indentations in the horizontal one (i.e. deposition direction). The deposition of the first layers of CuSn11 on C45 involves mixing these two materials because of the Marangoni and Buoyancy effects, as introduced previously. Figure 7 illustrates the results of a linear EDX analysis carried out on a one-layer sample. By examining Figure 7, it is possible to see the aforementioned material mixing. Therefore, the resulting mean value is higher than that observed in the five-layers sample.

The decrease in the five-layers sample is due to the greater quantity of bronze layers, which also allows for indentations in the region comprising solely bronze, characterized by a lower microhardness. The mixing of materials was confirmed by the EDX analysis of five-layers sample, whose images are shown in Figure 8. It is important to note, in particular, the presence of iron in the upper region, that is, the bronze one, and the presence of copper and tin in the bottom area, that is, the steel substrate.

Moreover, no detachments, cracks or porosities are found, as it is possible to see in the SEM image, reported in Figure 9, indicative of a sound deposition.

Three-point bending tests were used to investigate the bonding strength between the materials. An image of the tested specimens is shown in Figure 10.

The results of the bending tests are presented in Figure 11 and Table 1. A displacement threshold of approximately 21 mm was

Figure 8 EDX Analysis of the interface region in the five-layer samples

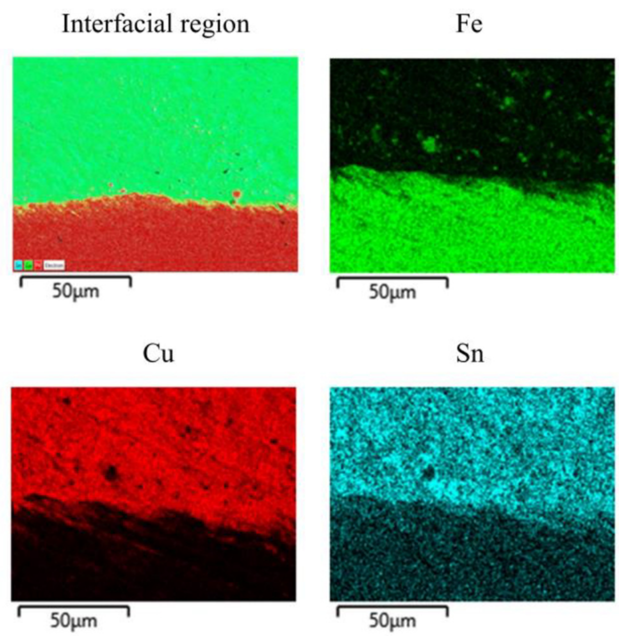

Source: Authors' own work

Figure 7 One-layer sample

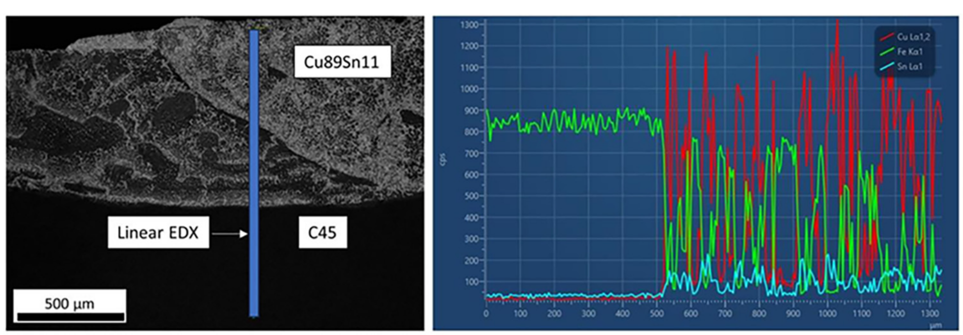

(a) (b)

Notes: (a) SEM image; (b) EDX spectrum for Fe (green line), Cu (red line) and Sn (blue line)
Source: Authors' own work

Figure 9 SEM Image of the five-layer sample at the steel/bronze interface

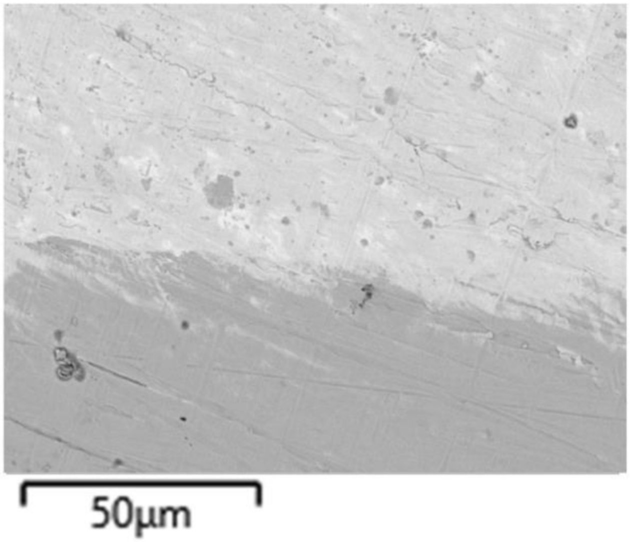

Source: Authors' own work

set as the displacement termination condition. A noteworthy observation can be made by examining the results. The flexural behavior of the bimetallic structure is contingent upon the positioning of the materials at the top and bottom. Specifically, when the bronze was positioned at the intrados and the steel at the extrados, the flexural strength was 993.5 ± 38.6 MPa, and all specimens reached a displacement of 21 mm, and although the specimens experienced severe deformation, no cracks or delamination were observed (as shown in Figure 12). These results

Figure 11 Flexural stress-displacement curves in three-point bending tests: continuous lines for CuSn11/C45 with CuSn11 at the top, dotted lines for CuSn11/C45 with C45 at the top

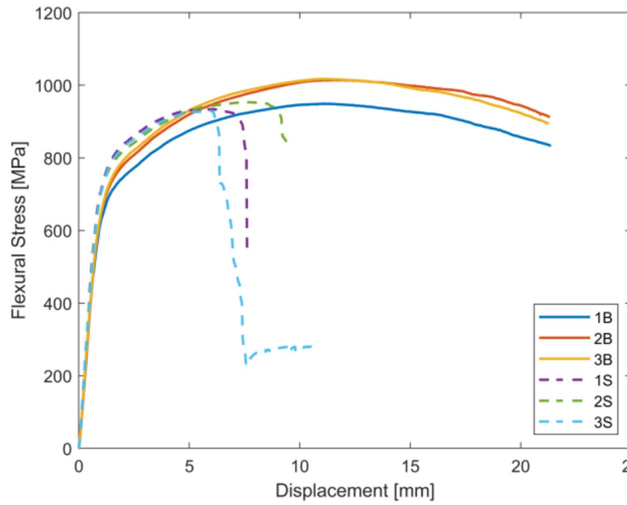

Source: Authors' own work

Table 1 Average values and standard deviation of ultimate flexural strength and displacement

Sample	Flexural strength (MPa)	Displacement (mm)
CuSn11 at the top	993.5 ± 38.6	21.3 ± 0.0 (threshold)
C45 at the top	938.7 ± 12.8	7.9 ± 1.4

Source: Authors' own work

Figure 10 Three-point bending test specimens

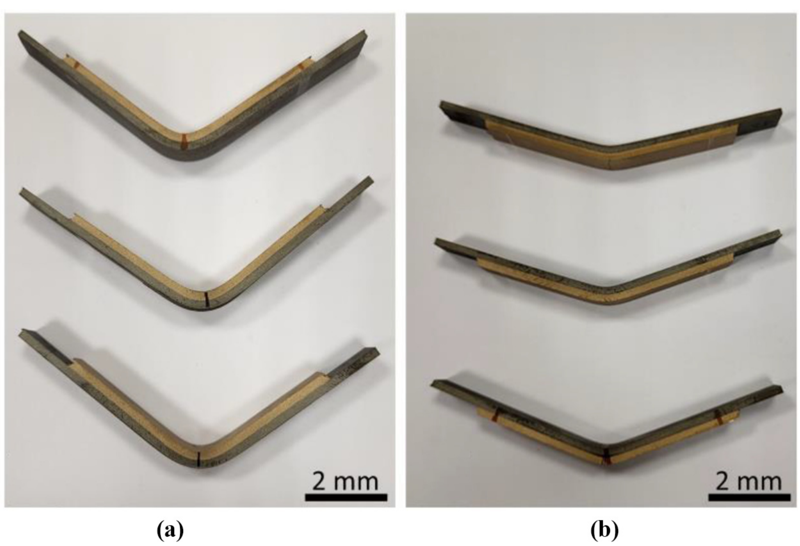

Notes: (a) CuSn11/C45 with CuSn11 at the top; (b) CuSn11/C45 with C45 at the top
Source: Authors' own work

Figure 12 Macrographs of the samples tested with bronze at the top

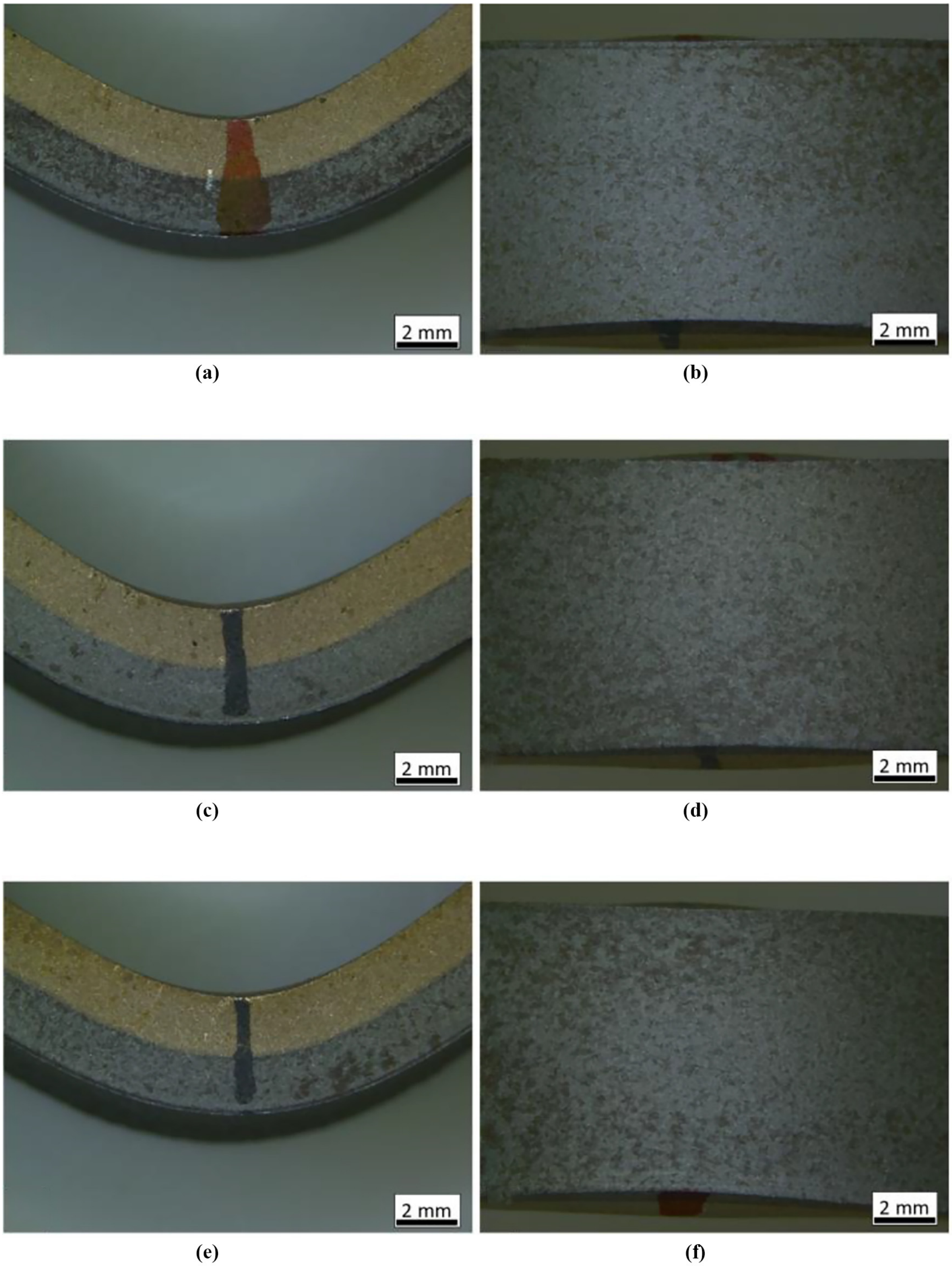

Notes: (a) side view of 1B; (b) bottom view of 1B; (c) side view of 2B; (d) bottom view of 2B; (e) side view of 3B; (f) bottom view of 3B
Source: Authors' own work

highlight the soundness of the material bonding between CuSn11 and C45, which is also demonstrated by the stable curve in the diagram shown in Figure 11 (B-samples are represented by the continuous lines). The graphs show no sharp changes or peaks, confirming the absence of cracking and delamination. Conversely, when CuSn11 was positioned at the bottom and the steel at the top, a slight decrease in the flexural strength was observed, i.e. 938.7 ± 12.8 MPa, and all specimens failed during the tests.

Figure 13 Macrographs of the samples tested with steel at the top

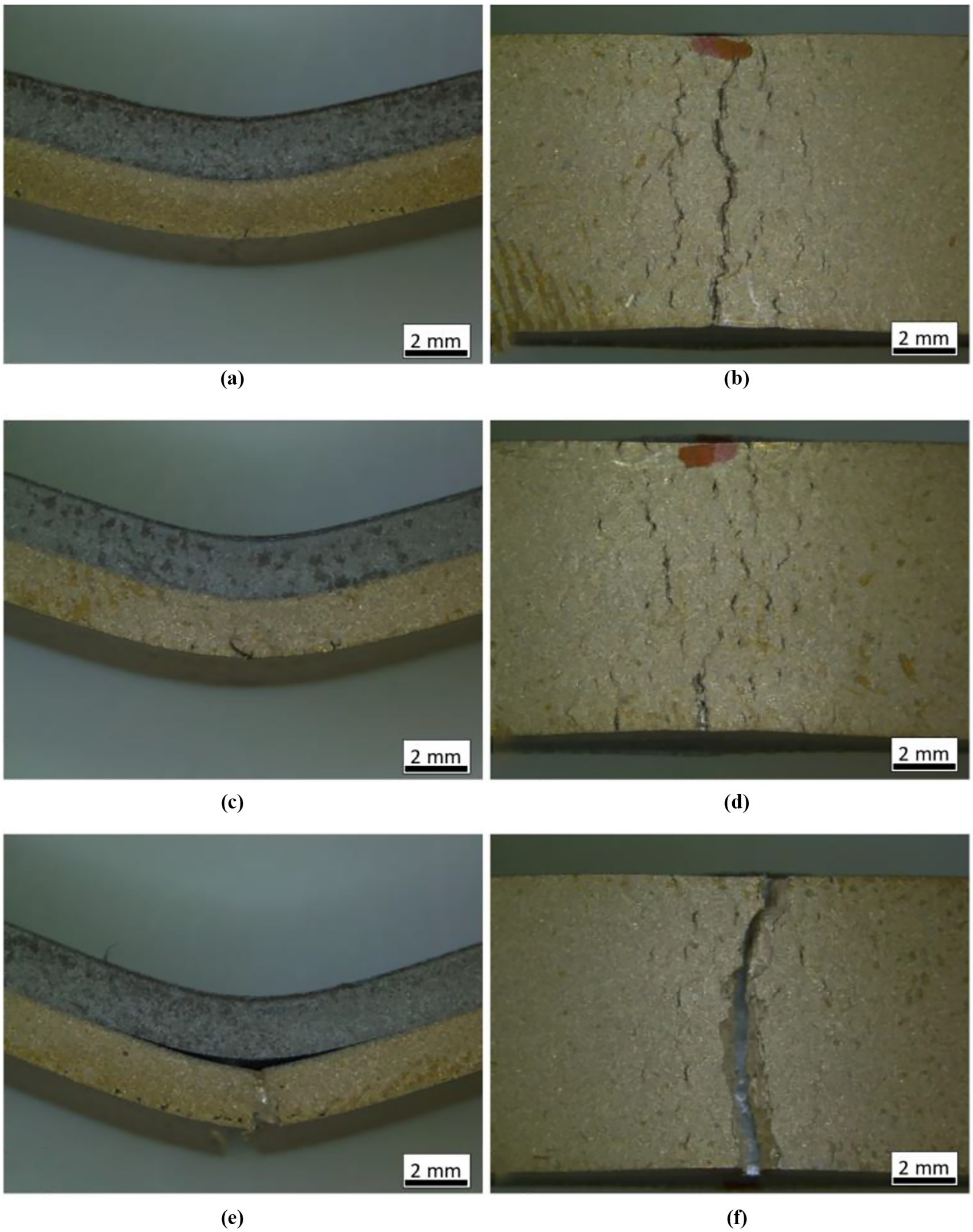

Notes: (a) side view of 1S; (b) bottom view of 1S; (c) side view of 2S; (d) bottom view of 2S; (e) side view of 3S; (f) bottom view of 3S
Source: Authors' own work

Additionally, the specimens exhibited more brittle behavior, leading to failure at a displacement of less than 50% of the imposed threshold (7.9 ± 1.4 mm), as shown in Figure 11 (S-samples are represented by the dotted lines). Figure 13 illustrates the side view of the S-samples and the bottom view, showing fractures in the bronze positioned at the bottom. It is important to note that for specimen 3S, the test was not stopped when the specimen failure started. Further considerations can be drawn from these premises. First, the fracture propagates in the same direction as the applied load, initially without delamination. Then, continuing to apply the load even after the initial failure, the fracture propagated along the direction of the load throughout the bronze region until it reached the steel region. At this point, the crack did not extend into the steel region, in agreement with Chen *et al.* (2019), but delamination occurred. In samples 1S and 2S, the crack occurred at the corner of the sample, where the sample is rounded, and the deformation is more severe, but no delamination followed. The fractures in the CuSn11 region in the S-samples can be attributed to the fact that in bimetal beams, the neutral axis shifts toward the material with a higher modulus of elasticity, which is higher for C45 compared to CuSn11 (approximately 220 GPa for C45 and 115 GPa for Bronze). Therefore, when the steel was positioned at the top, the neutral axis shifted upward, and consequently, the bronze was subjected to greater and more intensive tension compared to the one applied to the steel in the B-samples during the bending tests (where the neutral axis shifted downward). The different bending behaviors highlight the possibility of creating a sound bimetallic structure characterized by different properties, which could be used according to the intended purpose.

Regarding the pull-off adhesion tests, the mean value of adhesion strength recorded by the instrumentation, along with its standard deviation, is 16.3 ± 1.5 MPa. However, no detachment of the bronze coating occurred, indicating a glue failure and confirming the sound adhesion between the CuSn11 and C45 (Figure 14).

The results obtained suggested that process parameters can be used to print Cu89Sn11 properly and, therefore, fabricate the bimetallic bearings. However, the results also indicated that one and two layers of bronze were not sufficient; on these bases, two bimetallic bearings were manufactured through the deposition of five layers of bronze on the C45 substrate, specifically using the "spiral" deposition strategy. The as-built sample is shown in Figure 15(a). Then, the sample was subjected to the machining phase, resulting in the hemispherical shape visible in Figure 15(b). In this step, the centered hole for the lubricant was also created. The final significant result is the successful production of the two bi-metallic bearings.

The second component is a flat-face plain bearing, presented in Figure 16. Also in this case, it is possible to note that the bronze was successfully deposited and then subjected to the machining to include the features for the lubrication and to reach the desired surface finishing.

The two plain bearings were currently installed in an industrial system and are still working under very severe conditions.

4. Conclusions

The work presented in this paper proves that it is possible to deposit bronze (Cu89Sn11) to a C45 steel component using L-DED technology to obtain a bi-metallic plain bearing. The analyses carried out on the specimens showed that an excellent interface is formed between the two metals, without the presence of pores or cracks, but preserving mechanical properties. An increase in hardness can be seen near the interface due to the dilution of C45 within the bronze. The results of the three-point bending tests demonstrated an excellent material bonding when the CuSn11 was positioned at the bottom, with a flexural strength of 993.5 ± 38.6 MPa. In these cases, despite the severe deformation, no delamination or crack occurred. Conversely, bimetal structures with CuSn11 at the bottom showed a lower flexural strength (938.7 ± 12.8 MPa), with cracks throughout the bronze region and delamination, but the crack did not extend to the C45 region. The different bending behaviors highlight the possibility of creating a sound bimetallic structure characterized

Figure 14 Adhesion tests: bottom view of aluminum dollies after the tests

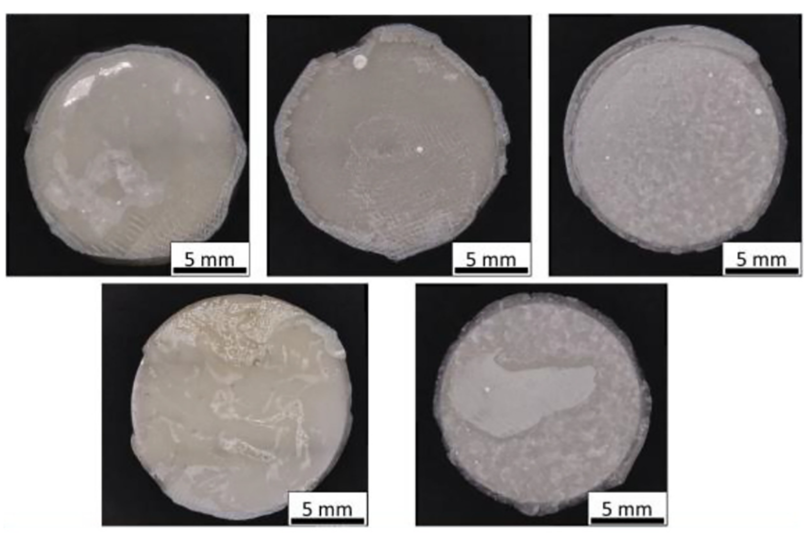

Source: Authors' own work

Figure 15 Hemispherical plain bearing obtained with the deposition of CuSn11 on a C45 substrate

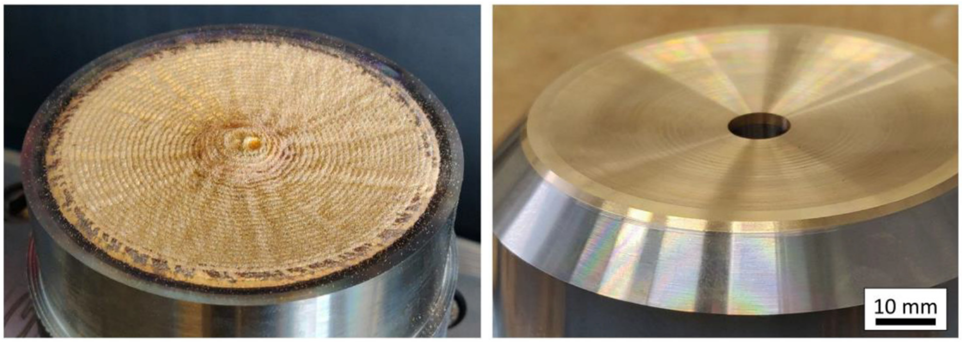

(a) **(b)**

Notes: (a) as- built; (b) machined
Source: Authors' own work

Figure 16 Flat-face plain bearing obtained with the deposition of CuSn11 on a C45 substrate, after machining

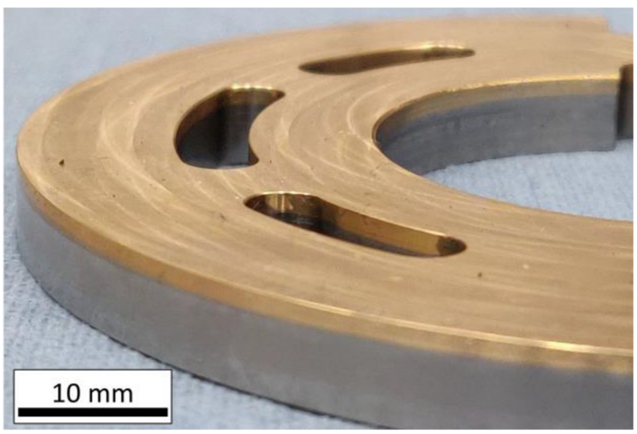

Source: Authors' own work

by different properties, which could be used according to the intended purpose.

Two types of bushings were deposited using the same process parameters as the five-layer specimen. In both cases, the bearings were successfully used in an industrial system after post-processing.

These results allow to widen the current fields of application of bi-metallic bearings by overcoming the issue associated with traditional manufacturing processes, exploiting the design freedom, the additive approach and the material mixing potential of the L-DED technology.

Ongoing activities are focused on the production of bimetallic plain bearings in functionally graded materials to improve the transition from one material to another.

References

ASTM D454-22 (2022), *ASTM D4541-22, Standard Test Method for Pull-off Strength of Coatings Using Portable Adhesion Testers*, *ASTM International*.

ASTM E92-82(2003) (2008), *Standard Test Method for Vickers Hardness of Metallic Materials*, *ASTM International*.

ASTM International (2002), "Standard test methods for flexural properties of unreinforced and reinforced plastics and electrical insulating materials. D790", *Annual Book of ASTM Standards*, pp. 1-12, doi: 10.1520/D0790-17.2.

ASTM International (2014), *ASTM B213: Standard Test Methods for Flow Rate of Metal Powders Using the Hall Flowmeter Funnel*, *Annual Book of ASTM Standards*.

Bandyopadhyay, A., Zhang, Y. and Onuike, B. (2022), "Additive manufacturing of bimetallic structures", *Virtual and Physical Prototyping*, Vol. 17 No. 2, doi: 10.1080/17452759.2022.2040738.

Chen, J., Yang, Y., Song, C., Zhang, M., Wu, S. and Wang, D. (2019), "Interfacial microstructure and mechanical properties of 316L/CuSn10 multi-material bimetallic structure fabricated by selective laser melting", *Materials Science and Engineering A*, Elsevier B.V, Vol. 752, pp. 75-85, doi: 10.1016/j.msea.2019.02.097.

Gibson, I., Rosen, D. and Stucker, B. (2015), "Directed energy deposition processes", *Additive Manufacturing Technologies: 3D Printing, Rapid Prototyping, and Direct Digital Manufacturing*, pp. 245-268, doi: 10.1007/978-1-4939-2113-3_10.

Hanon, M.M., Alshammas, Y. and Zsidai, L. (2020), "Effect of print orientation and bronze existence on tribological and mechanical properties of 3D-printed bronze/PLA composite", *The International Journal of Advanced Manufacturing Technology*, Vol. 108s No. 1-2, pp. 553-570, doi: 10.1007/s00170-020-05391-x.

Izadi, M., Farzaneh, A., Mohammed, M., Gibson, I. and Rolfe, B. (2020), "A review of laser engineered net shaping (LENS) build and process parameters of metallic parts", *Rapid Prototyping Journal*, Vol. 26 No. 6, doi: 10.1108/RPJ-04-2018-0088.

Joshi, G.R. and Badheka, V.J. (2019), "Processing of bimetallic steel-copper joint by laser beam welding", *Materials and Manufacturing Processes*, Vol. 34 No. 11, doi: 10.1080/10426914.2019.1628262.

Junghans, R., Neukirchner, J., Schumann, D. and Lippman, K. H. (1996), "The use of sintered metal bearings for high sliding velocities", *Tribology International*, Vol. 29 No. 3, pp. 181-192, doi: 10.1016/0301-679X(95)00087-K.

Kannan, R., Lee, Y., Pierce, D., Unocic, K., Fillingim, B., Feldhausen, T., Rossy, A.M., *et al.* (2023), "Additive manufacturing as a processing route for steel-aluminum bimetallic structures", *Materials & Design*, Vol. 231, doi: 10.1016/j.matdes.2023.112003.

Li, X.B., Zu, G.Y. and Wang, P. (2014), "Asymmetry in interface and bending property of Al/Cu/Al bimetallic laminates", *Rare Metals*, Vol. 33 No. 5, doi: 10.1007/s12598-014-0335-y.

Materials, T. (2004), *ASM Handbook*, *9*, *Metallography and Microstructures*, *Technology*.

Ovchinnikov, E.V., Leshchik, S.D., Struk, V.A., Kholodilov, O.V. and Fedorov, D.I. (2000), "Tribological characteristics of composite multilayered coatings", *Journal of Friction and Wear*.

Pratt, G.C. (1973), "Materials for plain bearings", *International Materials Reviews*, Vol. 18 No. 2, pp. 62-88, doi: 10.1179/imr.1973.18.2.62.

Pratt, G.C. (2001), "Bearing materials: plain bearings", *Encyclopedia of Materials: Science and Technology*, pp. 488-496, doi: 10.1016/b0-08-043152-6/00094-2.

Silvestri, A.T., Amirabdollahian, S., Perini, M., Bosetti, P. and Squillace, A. (2021), "Direct laser deposition for tailored structure", *Esaform 2021*, doi: 10.25518/esaform21.4124.

Silvestri, A.T., Bosetti, P. and Squillace, A. (2023), "Laser-Directed energy deposition of H13: processing window and improved characterization procedures", *Materials and Manufacturing Processes*, Taylor & Francis, Vol. 38 No. 14, pp. 1-15, doi: 10.1080/10426914.2023.2219302.

Sudhakar, K.V. (2002), "Failure analysis of automobile bimetal bearings", *Engineering Failure Analysis*, Vol. 9 No. 2, pp. 221-225, doi: 10.1016/S1350-6307(00)00048-0.

Summer, F., Grün, F., Offenbecher, M. and Taylor, S. (2019), "Challenges of friction reduction of engine plain bearings – tackling the problem with novel bearing materials", *Tribology International*, Vol. 131, pp. 238-250, doi: 10.1016/j.triboint.2018.10.042.

Tallafuss, P. and Johnston, J. (2018), "Defects, causes and prevention controls in the continuous bronze/steel bimetal strip sintering process", *Engineering Failure Analysis*, Elsevier, Vol. 92, pp. 32-43, doi: 10.1016/j.engfailanal.2018.05.003.

Thompson, S.M., Bian, L., Shamsaei, N. and Yadollahi, A. (2015), "An overview of direct laser deposition for additive manufacturing; part I: transport phenomena, modeling and diagnostics", *Additive Manufacturing*, Vol. 8, pp. 36-62, doi: 10.1016/j.addma.2015.07.001.

Topolski, K., Szulc, Z. and Garbacz, H. (2016), "Microstructure and properties of the Ti6Al4V/Inconel 625 bimetal obtained by explosive joining", *Journal of Materials Engineering and Performance*, Vol. 25 No. 8, doi: 10.1007/s11665-016-2080-x.

Valeeva, A.K., Valeev, I.S., Fazlyakhmetov, R.F., Barykin, N.P. and Reva, A.V. (2012), "Tin- and copper-based electrochemical coatings for sliding bearings", *Journal of Friction and Wear*, Vol. 33 No. 1, pp. 34-38, doi: 10.3103/S1068366612010126.

Wilson, R.W. and Shone, E.B. (1983), "The diagnosis of plain bearing failures", *Tribology Series*, Vol. 8 No. C, pp. 80-131, doi: 10.1016/S0167-8922(08)70695-3.

Zeidan, F.Y. and Herbage, B.S. (1991), "Fluid film bearing fundamentals and failure analysis", *Proceedings of the 20th Turbomachinery Symposium*, pp. 161-186.

Corresponding author

Alessia Teresa Silvestri can be contacted at: alessiateresa.silvestri@unina.it